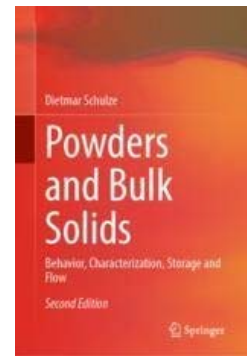


More information on flow properties and handling of powders and bulk solids can be found in:

**Powders and Bulk Solids**  
– Behavior, Characterization, Storage and Flow

by Dietmar Schulze

2nd ed. 2021, published by Springer  
(Link: <https://www.springer.com/us/book/9783030767198>)



## Flow Properties of Powders and Bulk Solids

Dietmar Schulze<sup>1</sup>

*In order to compare and optimize powders regarding flowability and to design powder handling equipment like silos, feeders, and flow promoting devices, it is necessary to know the mechanical properties – the so-called flow properties. In the present paper it is outlined which physical parameters describe the flow properties of a powder or a bulk solid, and how these parameters can be measured.*

### 1 Introduction

Knowledge of the flow properties of a powder or a bulk solid is necessary to design silos and other bulk solid handling equipment so that no flow problems (flow obstructions, segregation, irregular flow, flooding, etc.) occur. Furthermore, quantitative information regarding flowability of bulk products is required, e.g. as part of comparative tests (e.g. effect of flow agents or other additions on flow behavior) and quality control. The flow properties depend on several parameters, e.g.,

- particle size distribution,
- particle shape,
- chemical composition of the particles,
- moisture,
- temperature.

It is not possible to determine theoretically the flow behaviour of bulk solids in dependence of all these parameters. Even if this were possible, the expense for the determination of all parameters of influence would be very high. Thus, it is necessary, and also simpler, to determine the flow properties in appropriate testing devices.

The present paper deals with all kind of particulate solids, which are also called bulk solids, powders, or granulates. In the following the general expression “bulk solid” is used for all these products.

<sup>1</sup> Prof. Dr. Dietmar Schulze, Dr. Dietmar Schulze GmbH, Wolfenbüttel, Germany.  
E-Mail: [mail@dietmar-schulze.de](mailto:mail@dietmar-schulze.de), Internet: [www.dietmar-schulze.de](http://www.dietmar-schulze.de)

## 2 Stresses

Figure 1 shows a bulk solid element in a container (assumptions: infinite filling height, frictionless internal walls). In the vertical direction, positive normal stress ( $\sigma_v > 0$ , compressive stress) is exerted on the bulk solid. As a result, within the bulk solid (Fig. 1) a horizontal stress,  $\sigma_h$ , prevails which is smaller than the vertical stress,  $\sigma_v$ , exerted on the bulk solid from the top. The ratio of horizontal stress to vertical stress is the stress ratio,  $K$  (also known as  $\lambda$ ).

$$K = \sigma_h / \sigma_v \quad (1)$$

Typical values of  $K$  are between 0.3 and 0.6 [1].

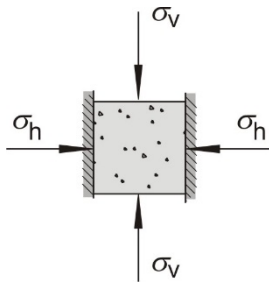


**Fig. 1:** Element of bulk solid

It follows that – in analogy to solids – in an element of bulk solid different stresses can be found in different cutting planes. Stresses in cutting planes other than the vertical and the horizontal can be analyzed using a simple equilibrium of forces.

No shear stresses  $\tau$  are exerted on the top or bottom surface of the bulk solid element in Fig. 1; i.e., the shear stresses in these planes are equal to zero. No shear stresses are acting at the lateral walls, since the lateral walls were assumed as frictionless. Thus, only the normal stresses shown are acting on the bulk solid from outside. Using a simple equilibrium of forces at a volume element with triangular cross-section cut from the bulk solid element shown in Fig. 1 (Fig. 2, on the left), the normal stress,  $\sigma_\alpha$ , and the shear stress,  $\tau_\alpha$ , acting on a plane inclined by an arbitrary angle  $\alpha$ , can be calculated. After some mathematical transformations it follows that:

$$\sigma_\alpha = \frac{\sigma_v + \sigma_h}{2} + \frac{\sigma_v - \sigma_h}{2} \cos(2\alpha) \quad (2)$$

$$\tau_\alpha = \frac{\sigma_v - \sigma_h}{2} \sin(2\alpha) \quad (3)$$

The pair of values  $(\sigma_\alpha, \tau_\alpha)$ , which are to be calculated according to equations (2) and (3) for all possible angles  $\alpha$ , can be plotted in a  $\sigma, \tau$ -diagram (normal stress, shear stress - diagram); see Fig. 2 on the right. If one joins all plotted pairs of values, a circle emerges; i.e., all calculated pairs of values form a circle in the  $\sigma, \tau$ -diagram.

This circle is called “the Mohr stress circle”. Its centre is located at  $\sigma_m = (\sigma_v + \sigma_h)/2$  and  $\tau_m = 0$ . The radius of the circle is  $\sigma_r = (\sigma_v - \sigma_h)/2$ . The Mohr stress circle represents the stresses on all cutting planes at arbitrary inclination angles  $\alpha$ , i.e., in all possible cutting planes within a bulk solid element.

Since the centre of the Mohr stress circle is always located on the  $\sigma$ -axis, each Mohr stress circle has two points of intersection with the  $\sigma$ -axis. The normal stresses defined through these

points of intersection are called the principal stresses, whereby the larger principal stress – the major principal stress – is designated as  $\sigma_1$  and the smaller principal stress – the minor principal stress – is designated as  $\sigma_2$ . If both principal stresses are given, the Mohr stress circle is well defined.

In the example of Fig. 1 both the horizontal and the vertical plane are free from shear stresses ( $\tau = 0$ ) and are thus principal stress planes. In this case the vertical stress,  $\sigma_v$ , which is greater than the horizontal stress,  $\sigma_h$ , is the major principal stress,  $\sigma_1$ , and the horizontal stress,  $\sigma_h$ , is the minor principal stress,  $\sigma_2$ .

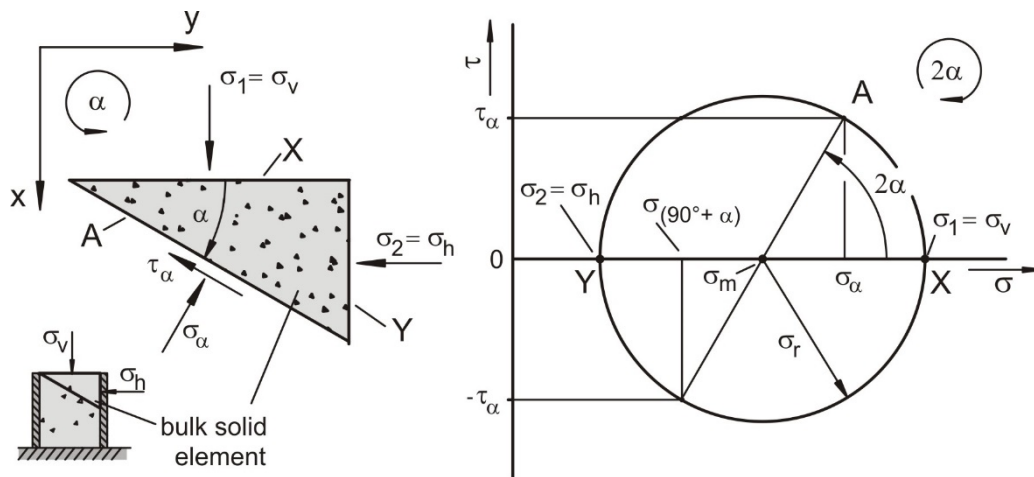


**Fig. 2:** Force equilibrium on an element of bulk solid, the Mohr stress circle

An important qualitative result of the above analysis is that shear stresses can occur in bulk solids at rest. This is impossible for a Newtonian fluid at rest (in contrast to Newtonian fluids, bulk solids can have sloped surfaces even at rest). Therefore, a representation of the stresses (fluids: pressures) in different cutting planes of a Newtonian fluid at rest in a  $\sigma, \tau$ -diagram would yield a stress circle with the radius zero (equation (3) with  $\sigma_h = \sigma_v$  yields  $\tau_\alpha = 0$ ).

From the explanation above it follows that the state of stress in a bulk solid cannot be completely described by only a single numerical value. Depending on the actual load acting on a bulk solid element, the corresponding Mohr stress circle can have a smaller or a larger radius, a centre at a lesser or greater normal stress, and hence also different principal stresses,  $\sigma_1$  and  $\sigma_2$ . In principle, at a given major principal stress,  $\sigma_1$ , stress circles with different values for the lowest principal stress,  $\sigma_2$ , are imaginable. Therefore, a stress circle is defined clearly only if at least two numerical values are given, i.e.,  $\sigma_1$  and  $\sigma_2$ .

In summary, the following can be stated with regard to the stresses acting in bulk solids:

- A bulk solid can transmit shear stresses even if it is at rest.
- In different cutting planes different stresses are acting.
- Stress conditions can be represented with Mohr stress circles.

### 3 Adhesive forces

The flowability of a bulk solid depends on the adhesive forces between individual particles. Different mechanisms create adhesive forces [2]. With fine-grained, dry bulk solids, adhesive forces due to van der Waals interactions play the essential role. With moist bulk solids, liquid bridges between the particles usually are most important. Liquid bridges are formed by small regions of liquid in the contact area of particles. The adhesion is a result of surface tension and capillary pressure.

Both types of adhesive forces described above are dependent on the distance between particles and on particle size.

Some bulk solids continue to gain strength if stored at rest under compressive stress for a longer time interval. This effect is called time consolidation. The reasons for time consolidation are also to be found in the effects of adhesive forces. Possible mechanisms are:

- Solids bridges due to solid crystallizing when drying moist bulk solids, where the moisture is a solution of a solid and a solvent [2] (e.g. sand and salt water).
- Solid bridges from the particle material itself, e.g. after some material at the contact points has been dissolved by moisture [2, 3] (e.g. crystal sugars with slight dampness).
- Bridges due to sintering during storage of the bulk solid at temperatures not much lower than the melting temperature [2]. This can appear e.g. at ambient temperature during the storage of plastics with low melting points.
- Plastic deformation at the particle contacts, which leads to an increase in the adhesive forces through approach of the particles and enlargement of the contact areas.
- Chemical processes (chemical reactions at the particle contacts).
- Biological processes (e.g. due to fungal growth on biologically active ingredients).

Whether a bulk solid flows well or poorly depends on the relationship of the adhesive forces to the other forces acting on the bulk solid. It can be shown that the influence of adhesive forces on flow behaviour increases with decreasing particle size. Thus, as a rule, a bulk solid flows more poorly with decreasing particle size. Fine-grained bulk solids with moderate or poor flow behaviour due to adhesive forces are called cohesive bulk solids.

If particles are pressed against each other by external forces, the compressive force acting between the particles increases. Thereby large stresses prevail (locally) at the particles' contact points, because the contact points are very small. This leads to plastic deformation of the particles in the contact area, so that the contact areas increase and the particles approach each other. Thereby the adhesive forces increase. Thus, a compressive force acting from outside on a bulk solid element can increase the adhesive forces. This mechanism is used e.g. in the production of tablets or briquettes.

The dependence of the adhesive forces between the particles on external forces exerted on a bulk solid is characteristic of bulk solids, especially for cohesive bulk solids. Therefore, an evaluation of bulk solids behaviour must always take into consideration the forces or stresses previously acting on the bulk solid, the stress history. The stress history includes, for example, the consolidation stress exerted on a bulk solid, leading to certain adhesive forces and hence to a certain strength of the bulk solid (e.g., the strength of a tablet is dependent on the maximum consolidation stress at tableting).

## 4 Flowability

### 4.1 Uniaxial compression test as model for explanation

The phrase “good flow behaviour” usually means that a bulk solid flows easily, i.e., it does not consolidate much and flows out of a silo or a hopper due to the force of gravity alone and no flow promoting devices are required. Products are “poorly flowing” if they experience flow obstructions or consolidate during storage or transport. In contrast to these qualitative statements, a quantitative statement on flowability is possible only if one uses an objective characteristic value that considers those physical characteristics of the bulk solid that are responsible for its flow behaviour.

“Flow” means that a bulk solid is deformed plastically due to the loads acting on it (e.g. failure of a previously consolidated bulk solid specimen). The magnitude of the load necessary for flow is a measure of flowability. This will be demonstrated first with the uniaxial

compression test. Figure 3 shows a hollow cylinder filled with a fine-grained bulk solid (cross-sectional area  $A$ ; internal wall of the hollow cylinder assumed as frictionless). The bulk solid is loaded by the stress  $\sigma_1$  – the consolidation stress – in the vertical direction. The more the volume of the bulk solid specimen is reduced, the more compressible the bulk solid is.

In addition to the increase in bulk density from consolidation stress, one will observe also an increase in strength of the bulk solid specimen. Hence, the bulk solid is both consolidated and compressed through the effect of the consolidation stress.

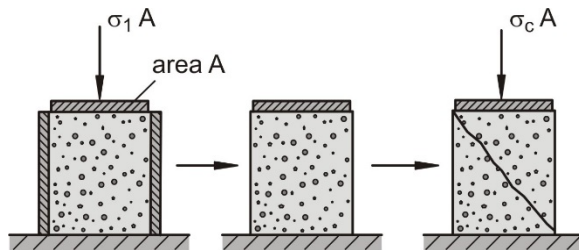


**Fig. 3:** Uniaxial compression test

After consolidation, the bulk solid specimen is relieved of the consolidation stress,  $\sigma_1$ , and the hollow cylinder is removed. If subsequently the consolidated cylindrical bulk solid specimen is loaded with an increasing vertical compressive stress, the specimen will break (fail) at a certain stress. The stress causing failure is called compressive strength or unconfined yield strength,  $\sigma_c$  (another common designation is  $f_c$ ).

In bulk solids technology one calls the failure “incipient flow”, because at failure the consolidated bulk solid specimen starts to flow. Thereby the bulk solid dilates somewhat in the region of the surface of the fracture, since the distances between individual particles increase. Therefore, incipient flow is plastic deformation with decrease of bulk density. Since the bulk solid fails only at a sufficiently large vertical stress, which is equal to the compressive strength, there must exist a material-specific yield limit for the bulk solid. Only when this yield limit is reached does the bulk solid start to flow.

The yield limits of many materials (e.g. metals) are material-dependent and are listed in tables. However, the yield limit of a bulk solid is dependent also on its stress history, i.e., previous consolidation: The greater the consolidation stress,  $\sigma_1$ , the greater the bulk density,  $\rho_b$ , and unconfined yield strength,  $\sigma_c$ .

Uniaxial compression tests (Fig. 3) conducted at different consolidation stresses,  $\sigma_1$ , lead to different pairs of values  $(\sigma_c, \sigma_1)$  and  $(\rho_b, \sigma_1)$ . Plotting these pairs of values as points in a  $\sigma_c, \sigma_1$ -diagram and a  $\rho_b, \sigma_1$ -diagram, respectively, and drawing in each diagram a curve through these points, usually results in curves like those for product A in Fig. 4, where bulk density,  $\rho_b$ , and unconfined yield strength,  $\sigma_c$ , typically increase with consolidation stress,  $\sigma_1$ . Very rarely a progressive slope like in the left part of curve B is observed. The curve  $\sigma_c(\sigma_1)$  is called the flow function, or, to express that it represents the behaviour at a very small consolidation time  $t \rightarrow 0$ , the instantaneous flow function.

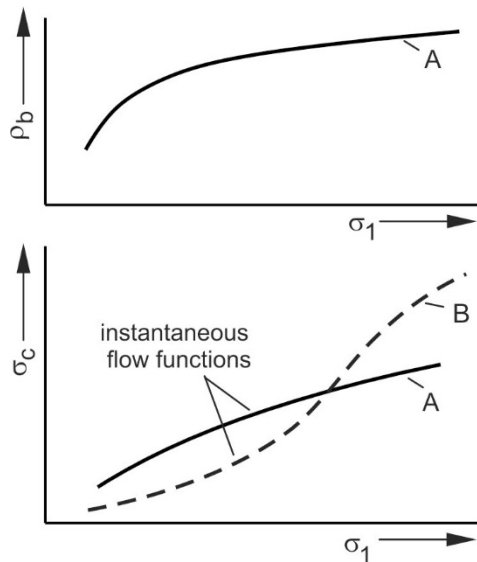


**Fig. 4:** Bulk density,  $\rho_b$ , and unconfined yield strength,  $\sigma_c$ , vs. consolidation stress,  $\sigma_1$

## 4.2 Time consolidation (caking)

Some bulk solids increase in strength if they are stored for a longer time at rest under a compressive stress (e.g. in a silo or an intermediate bulk container). This effect is called time consolidation or caking. Time consolidation can be determined with the test shown in Fig. 3, in order, e.g., to simulate long-term storage in a silo. For this one loads the specimen with consolidation stress,  $\sigma_1$ , not only for a short moment, but for a defined period,  $t_1$ . Then the unconfined yield strength is determined following the principle explained above (Fig. 3).

Figure 5 shows the flow function  $\sigma_c(\sigma_1)$  of product A as previously shown in Fig. 4 (unconfined yield strength without influence of time consolidation, i.e., for a storage period  $t = 0$ ). Additionally, examples of curves  $\sigma_c(\sigma_1)$  for storage periods  $t > 0$  (curves  $A_1$ ,  $A_2$ ) are drawn. The curves  $\sigma_c(\sigma_1)$  for the storage periods  $t > 0$  are called time flow functions. Here each curve emerges from the connection of several pairs of values  $(\sigma_c, \sigma_1)$ , which were measured at identical storage periods,  $t$ , but at different consolidation stresses,  $\sigma_1$ .

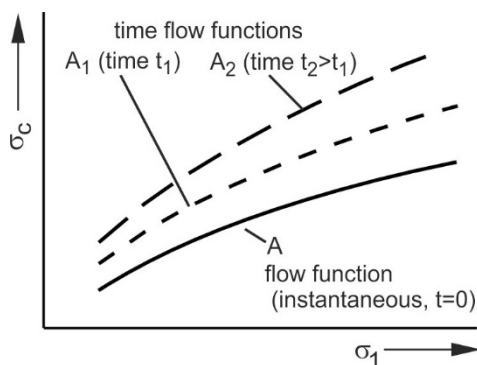


**Fig. 5:** Flow function and time flow functions for two different storage times  $t_1$  and  $t_2 > t_1$ .

For the example of bulk solid A, the unconfined yield strength,  $\sigma_c$ , increases with increasing storage time. This result is true for many bulk solids, but not for all. There are bulk solids which undergo no or only very slight consolidation over time; i.e.,  $\sigma_c$  does not increase, or increases only very slightly with increasing storage period,  $t$  (e.g. dry quartz sand). Other bulk solids undergo a large increase in unconfined yield strength after storage periods of only a few hours, whereas after longer storage periods their unconfined yield strength does not increase further.

These differences are due to the different physical, chemical, or biological effects that are the causes of consolidation over time, e.g. chemical processes, crystallizations between the particles, enlargement of the contact areas through plastic deformation, capillary condensation, or biological processes such as fungal growth (see Section 3).

With measurement of time consolidation, a “time-lapse effect” is not realizable; i.e., one must store a bulk solid specimen at the consolidation stress,  $\sigma_1$ , for exactly that period of time for which one would like to get data on time consolidation. Without such a test no quantitative statement can be made regarding time consolidation.

### 4.3 Yield limit and Mohr stress circles

The uniaxial compression test presented in Fig. 3 is shown below in a  $\sigma, \tau$ -diagram (Fig. 6). If one neglects the force of gravity of the bulk solid specimen and assumes that no friction is acting between the wall of the hollow cylinder and the bulk solid, both vertical stress,  $\sigma_v$ , as well as horizontal stress,  $\sigma_h$ , are constant within the entire bulk solid specimen. Therefore, at each position in the bulk solid sample the state of stress, which can be represented by a Mohr stress circle, is identical.

During consolidation the vertical normal stress,  $\sigma_1$ , acts on the top of the bulk solid specimen. Perpendicular to the vertical stress the lesser, horizontal stress prevails according to stress ratio  $K$  (see Section 2). Neither at top nor at bottom of the specimen, nor at the internal wall of the hollow cylinder, which is assumed as frictionless, will shear stresses be found; i.e.,  $\tau = 0$ . The pairs of values  $(\sigma, \tau)$  for vertical and horizontal cutting planes within the bulk solid specimen are plotted in the  $\sigma, \tau$ -diagram (Fig. 6). Both points are located on the  $\sigma$ -axis because  $\tau = 0$ . The Mohr stress circle A, which describes the stresses in the bulk solid sample at consolidation, is thus well defined (because each stress circle has exactly two intersections with the  $\sigma$ -axis).

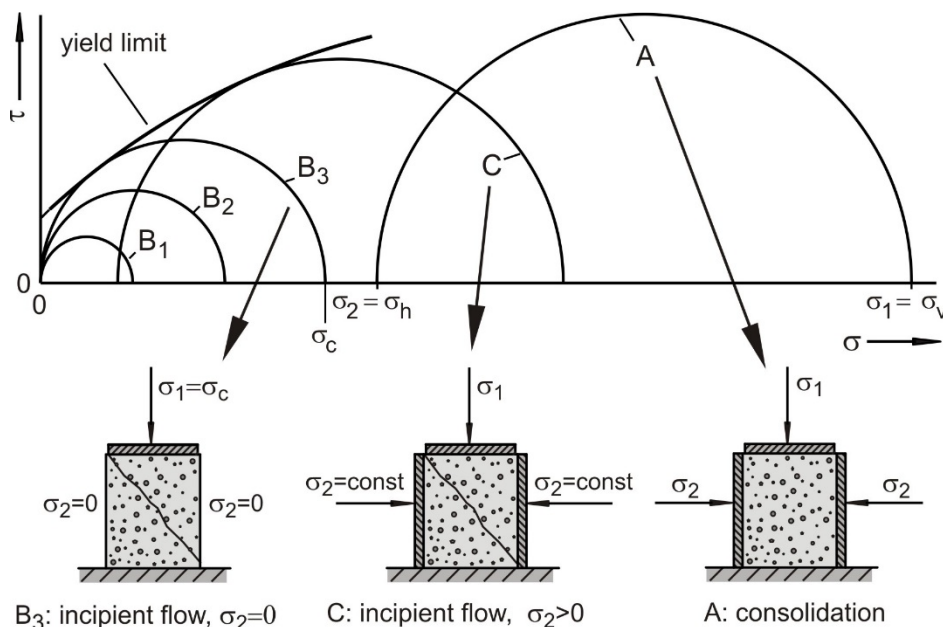


**Fig. 6:** Measurement of unconfined yield strength in a  $\sigma, \tau$ -diagram

Since in the vertical plane the shear stress is zero, the vertical stress is identical with the major principal stress,  $\sigma_1$  (see Section 2: Principal stresses are the normal stresses in those planes in which the shear stresses are equal to zero). The major principal stress,  $\sigma_1$ , is equal to the vertical stress,  $\sigma_v$ , and the minor principal stress,  $\sigma_2$ , is equal to the horizontal stress,  $\sigma_h$ .

In the second part of the test shown in Fig. 3, the specimen is loaded with increasing vertical stress after it has been relieved of the consolidation stress and the hollow cylinder has been removed. The vertical stress and horizontal stress are principal stresses. The horizontal stress is independent of the vertical load equal to zero, since the lateral surface of the specimen is uncovered and not loaded.

During the increasing vertical load in the second part of the test, the stress states at different load steps are represented by stress circles with increasing diameter (stress circles  $B_1$ ,  $B_2$ ,  $B_3$  in Fig. 6). The lesser principal stress, which is equal to the horizontal stress, is equal to zero at all stress circles.

At failure of the specimen the Mohr stress circle  $B_3$  represents the stresses in the bulk solid sample. Since the load corresponding to this Mohr stress circle causes incipient flow of the specimen, the yield limit of the bulk solid must have been attained in one cutting plane of the specimen. Thus, Mohr stress circle  $B_3$  must reach the yield limit in the  $\sigma, \tau$ -diagram. In Fig. 6 a possible yield limit is shown. The real course of the yield limit can not be determined with only the uniaxial compression test.

The Mohr stress circles  $B_1$  and  $B_2$ , which are completely below the yield limit, cause only an elastic deformation of the bulk solid specimen, but no failure and/or flow. Stress circles larger than stress circle  $B_3$ , and thus partly above the yield limit, are not possible: The specimen would already be flowing when the Mohr stress circle reaches the yield limit (failure), so that no larger load could be exerted on the specimen.

If, during the second part of the experiment shown in Fig. 3 (measurement of compressive strength), one were to apply also a constant horizontal stress  $\sigma_h > 0$  on the specimen (in addition to the vertical stress,  $\sigma_v$ ), one would likewise find stress circles that indicate failure of the specimen and reach the yield limit (e.g. stress circle C in Fig. 6). Thus, the yield limit is the envelope of all stress circles that indicate failure of a bulk solid sample.

#### 4.4 Numerical characterization of flowability

Flowability of a bulk solid is characterized mainly by its unconfined yield strength,  $\sigma_c$ , in dependence on consolidation stress,  $\sigma_1$ , and storage period,  $t$ . Usually the ratio  $ff_c$  of consolidation stress,  $\sigma_1$ , to unconfined yield strength,  $\sigma_c$ , is used to characterize flowability numerically:

$$ff_c = \sigma_1 / \sigma_c \quad (4)$$

The larger  $ff_c$  is, i.e., the smaller the ratio of the unconfined yield strength,  $\sigma_c$ , to the consolidation stress,  $\sigma_1$ , the better a bulk solid flows. Similar to the classification used by Jenike [4], one can define flow behaviour as follows:

$ff_c < 1$	not flowing
$1 < ff_c < 2$	very cohesive
$2 < ff_c < 4$	cohesive
$4 < ff_c < 10$	easy-flowing
$10 < ff_c$	free-flowing



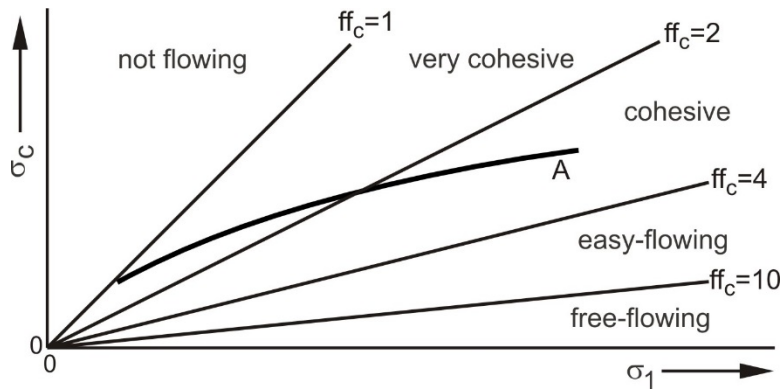


**Fig. 7:** Flow function and lines of constant flowability

In Fig. 7 the flow function A taken from the  $\sigma_c, \sigma_1$ -diagram in Fig. 4 are shown. Additionally, the boundaries of the ranges of the classifications listed above are shown as straight lines, each representing a constant value of flowability,  $ff_c$ . This diagram clearly shows that the flowability,  $ff_c$ , of a specific bulk solid is dependent on the consolidation stress,  $\sigma_1$  (in most cases  $ff_c$  increases with  $\sigma_1$  as with bulk solid A). Therefore, with each consolidation stress at which  $\sigma_c$  and thus  $ff_c$  were determined, one obtains a different value of flowability: The flowability of a bulk solid depends on the stress level (= consolidation stress); thus for most bulk solids one will obtain a larger value of flowability (= better flowability) at a greater consolidation stress. For most bulk solids one will find a (possibly extremely low) consolidation stress at which the bulk solid flows poorly. Because of the dependence of flowability on consolidation stress, it is not possible (unfortunately!) to describe the flowability of a bulk solid with only one numerical value.

With the results of time consolidation tests, flowability can be determined with Eq. (4), using the unconfined yield strength,  $\sigma_c$ , which was measured after the corresponding storage period. If the bulk solid shows a time consolidation effect, one will measure an increasing unconfined yield strength with increasing storage period, so that from Eq. (4) a smaller flowability will follow. This is to be expected: If a bulk solid gains strength with an increasing period of storage at rest at a certain consolidation stress, it will be more difficult to get this bulk solid to flow; i.e., its flowability decreases with increasing storage period.

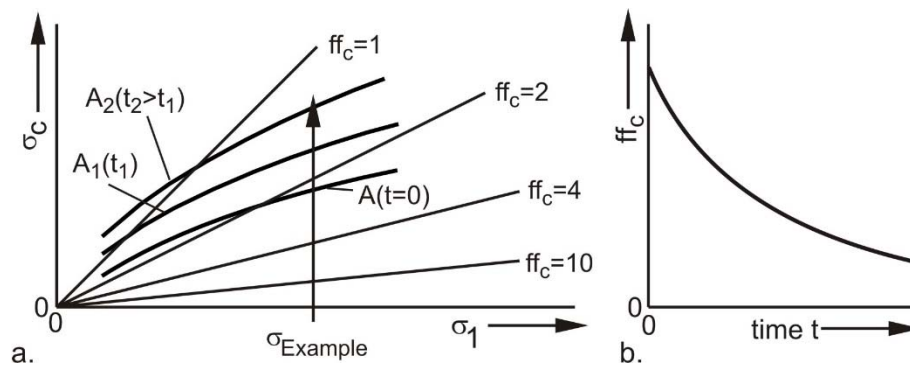


**Fig. 8:** Influence of storage time on flowability

In Fig. 8.a flow function A and two time flow functions taken from Fig. 5 are shown. The flow function represents unconfined yield strength,  $\sigma_c$ , in dependence on consolidation stress,  $\sigma_1$ , without influence of a storage period, i.e., for the storage period  $t = 0$ . A time flow function represents the unconfined yield strength which emerges after storage at the consolidation stress over a period,  $t$ . Further, as in Fig. 7, the boundaries of the ranges following from the classification of flowability are plotted. It can be seen that flowabilities,  $ff_c$ , measured at identical consolidation stress, but after different consolidation periods, decrease with increasing consolidation time (Fig. 8b). For the consolidation stress,  $\sigma_{\text{Example}}$ , chosen as an example, one obtains

measurement points in areas of decreasing flowability when increasing the consolidation period  $t$  (see arrow in Fig. 8a).

From the dependence of flowability,  $ff_c$ , on consolidation stress,  $\sigma_1$ , it follows that one can compare the flow behaviour of several bulk solids quantitatively using  $ff_c$  only if all measurements have been performed at identical consolidation stresses. Otherwise totally different (incorrect) statements might result. This shows how important it is to test a bulk solid at defined and known conditions (e.g. known consolidation stress).

## 5 Practical determination of flow properties

In the previous section the flow behaviour has been explained in a simplified way by using the uniaxial compression test as a model. The use of the uniaxial compression test with fine-grained, cohesive bulk solids is problematic, because one obtains unconfined yield strength values that are too low [7], and preparation of the hollow cylinder to obtain frictionless walls is very time-consuming. In addition, further important parameters (e.g. internal friction and wall friction) cannot be determined with this test. It is, however, an appropriate measurement technique for the measurement of the time consolidation of coarse-grained bulk solids.

In order to measure the flow properties of fine-grained bulk solids, in advanced bulk solids technology so-called shear testers are used. In the following first the principle of shear testing is outlined. Afterwards, the translational shear tester introduced by Jenike around 1960 (Jenike shear tester; the first shear tester especially designed for bulk solids) [2, 4, 6–8] and the Schulze ring shear tester [6, 9–13] will be described.

### 5.1 Shear test procedure (yield locus)

The goal of a shear test is to measure the yield limit of a consolidated bulk solid. The yield limit is called yield locus in bulk solids technology. For a shear test, a bulk solid specimen is loaded vertically by a normal stress,  $\sigma$  (Fig. 9a). Then a shear deformation is applied on the specimen by moving the top platen with a constant velocity,  $v$ . This results in a horizontal shear stress,  $\tau$  (Fig. 9b). With increasing shear stress the resultant force,  $F_R$ , acting on the bulk solid specimen, increases.

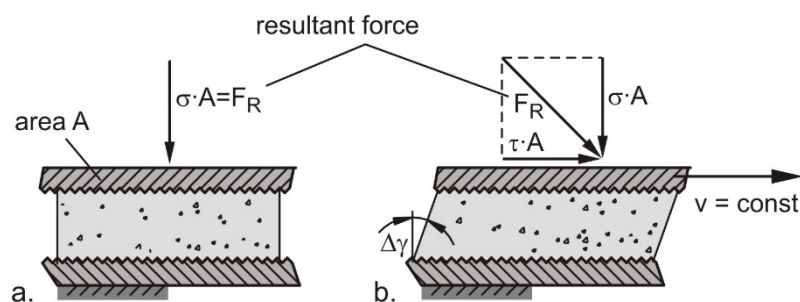


**Fig. 9:** Bulk solid specimen: a. initial loading with normal stress  $\sigma$ ; b. shear deformation (velocity  $v = \text{const}$ )

When a point of a yield locus is measured, in analogy to the uniaxial compression test, two steps are necessary: First the bulk solid specimen is consolidated, what is called “preshear”. Subsequently a point of the yield limit is measured. This step is called “shear” or “shear to failure”.

For preshear the bulk solid specimen is loaded in the vertical direction by a well-defined normal stress,  $\sigma = \sigma_{\text{pre}}$ . Then the specimen is sheared. At the beginning of preshear the shear stress  $\tau$  increases with time (as shown in the left diagram in Fig. 10). With time the curve of

shear stress vs. time becomes flatter, and finally the shear stress remains constant even though the specimen is sheared further. The constant shear stress is called  $\tau_{pre}$ . After constant shear stress has been attained, neither shear resistance (and strength) nor bulk density increase further. Thus, the bulk solid specimen is sheared at constant normal stress,  $\sigma$ , constant shear stress,  $\tau$ , and constant bulk density,  $\rho_b$ . Thus flow, or plastic deformation, occurs at constant bulk density. This type of flow, attained at preshear, is called steady-state flow. The state of the bulk solid after steady-state flow is attained is called “critically consolidated with respect to normal stress,  $\sigma_{pre}$ ”. The characteristic stress for this consolidation – the major principal stress  $\sigma_1$  – will be considered later.

The bulk density,  $\rho_b$ , and the shear stress,  $\tau_{pre}$ , attained at steady-state flow are characteristic for the applied normal stress at preshear,  $\sigma_{pre}$ . In principle, an identical state of consolidation, characterized by the same bulk density,  $\rho_b$ , and the same shear stress,  $\tau_{pre}$ , will be attained with other specimens of the same bulk solid presheared under the same normal stress,  $\sigma_{pre}$ .

After the bulk solid specimen has been consolidated by the preshear procedure, the shear deformation is reversed until the shear stress,  $\tau$ , is reduced to zero. The pair of values of normal stress and shear stress at steady-state flow ( $\sigma_{pre}$ ,  $\tau_{pre}$ ) is plotted in a normal stress - shear stress diagram ( $\sigma, \tau$ -diagram, Fig. 10, right). Point ( $\sigma_{pre}$ ,  $\tau_{pre}$ ) is called the “preshear point”.

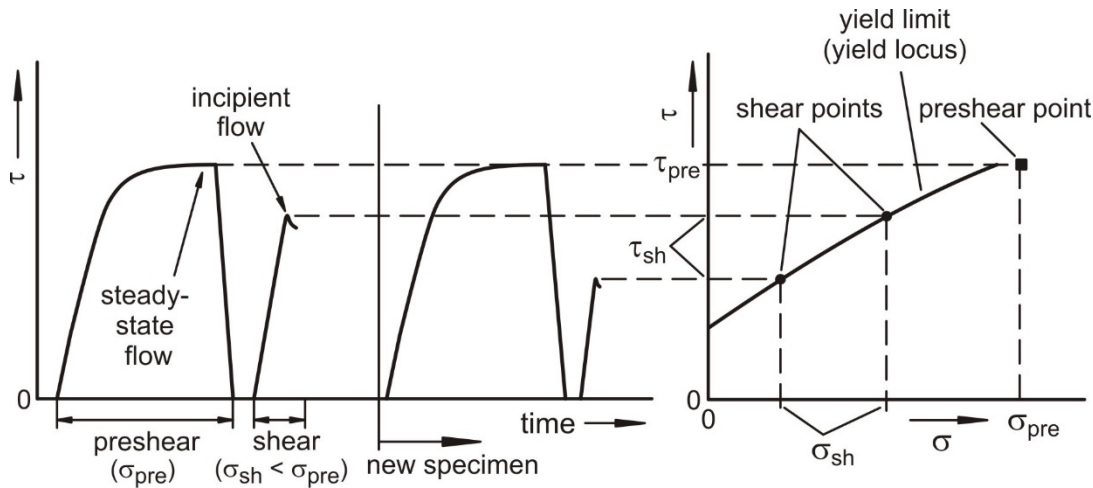


**Fig. 10:** Plot of shear stress vs. time; yield locus

After preshear the bulk solid specimen in the shear cell is defined as a critically consolidated specimen. The second step of the test procedure – shear or shear to failure – is discussed next.

For shear to failure the normal stress acting on the specimen is decreased to a value  $\sigma_{sh}$ , which is less than the normal stress at preshear,  $\sigma_{pre}$ . Had the specimen been presheared under the lower normal stress,  $\sigma_{sh}$ , and not under  $\sigma_{pre}$ , its bulk density and strength would have been less. Since the specimen was presheared under the greater normal load,  $\sigma_{pre}$ , it was consolidated more than it would have been with the lower normal load,  $\sigma_{sh}$ .

If the consolidated specimen is sheared under the normal stress  $\sigma_{sh} < \sigma_{pre}$ , it will start to flow (fail) when a sufficiently large shear force, or shear stress, is attained. At that point particles start to move against each other. The material will start to dilate (decrease in bulk density) and shear resistance and thus shear stress will decrease (Fig. 10). The maximum shear stress characterizes incipient flow. The corresponding pair of values ( $\sigma_{sh}$ ,  $\tau_{sh}$ ) is a point of the yield limit of the consolidated specimen in the  $\sigma, \tau$ -diagram (Fig. 10, right). Such a point is called a “shear point” or a “point of incipient flow”.

In order to measure the course of the yield locus, several of the tests described above must be performed, where the specimens first must be consolidated at identical normal stress,  $\sigma_{pre}$  (preshear). Then the specimens are sheared (to failure) under different normal stresses,  $\sigma_{sh} < \sigma_{pre}$ . As outlined above, by preshearing at identical normal stress,  $\sigma_{pre}$ , each specimen

reaches the same state of consolidation. Each test yields the same preshear point ( $\sigma_{pre}$ ,  $\tau_{pre}$ ), and one individual shear point ( $\sigma_{sh}$ ,  $\tau_{sh}$ ) in accordance with the different normal stresses,  $\sigma_{sh}$ , applied at shear. The yield locus follows from a curve plotted through all measured shear points (Fig. 10, right).

## 5.2 Jenike shear tester

Around 1960 Jenike [4] published his fundamental work on silo and bulk solids technology and introduced the Jenike Shear Tester, a translational shear tester. This tester was the first one designed for the purposes of powder technology.

The shear cell of the Jenike shear tester consists of a bottom ring (also called mould ring), a ring of the same diameter (so-called upper ring) lying above the bottom ring, and a lid (Fig. 11). The lid is loaded centrally with a normal force,  $F_N$ . The upper part of the shear cell is displaced horizontally against the fixed bottom ring by a motor driven stem which pushes against a bracket fixed to the lid. The force  $F_S$  – the shear force – exerted by the stem is measured. Due to the displacement of the upper ring and the lid against the bottom ring, the bulk solid undergoes a shear deformation. The normal stress,  $\sigma$ , and shear stress,  $\tau$ , acting in the horizontal plane between upper ring and bottom ring are determined by dividing normal force,  $F_N$ , and shear force,  $F_S$ , by the cross-sectional area of the shear cell,  $A$ .

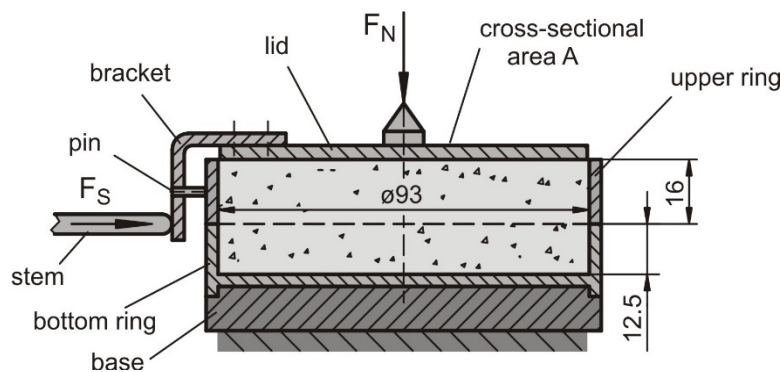


**Fig. 11:** Shear cell of the Jenike shear tester [4, 7, 8]

For the measurement of a point of a yield locus, the shear cell is filled with the bulk solid specimen. After a manual preconsolidation [7, 8] the specimen is presheared and then sheared to failure as outlined in the previous section. For the next point of the yield locus, a new bulk solid specimen has to be prepared and sheared.

Although the Jenike Shear Tester is internationally recognized, from today's point of view a disadvantage might be the time required for a test (one to two hours per yield locus; depending on the powder and the operator's skill) during which the operator has to be present. In addition, the manual preconsolidation of each specimen can be a source of measurement errors, and due to the limited shear displacement (maximum: twice the thickness of the wall of the upper ring) materials requiring too much deformation to attain steady-state flow can hardly be tested.

## 5.3 Ring shear tester

Ring shear testers (rotational shear testers) have been used in soil mechanics since the 1930s [14]. In the 1960s Walker designed a ring shear tester for bulk solids [15], where lower stresses than in soil mechanics are of interest. In the following decades different ring shear testers have been built and investigated at several universities (e.g. [16, 17]). In 1992 a ring shear tester (type RST-01.01, standard specimen volume 900 ml, optionally smaller shear cells can be used)

[9, 10] was developed by the author, followed by a computer-controlled version of this tester in 1997 (type RST-01.pc). It is connected to a personal computer running a control software. With this control software yield loci, wall yield loci, time consolidation, etc. can be measured automatically. A smaller computer-controlled ring shear tester (type RST-XS) has been available since 2002, its successor presented in 2013 is the even smaller ring shear tester RST-XS.s. These testers can be used with shear cells of small specimen volumes from 3.5 ml to 70 ml.

Figure 12 shows the principle of the shear cell of a ring shear tester (series RST-01) [6, 9, 10, 13]. The ring-shaped (annular) bottom ring of the shear cell contains the bulk solid specimen. The (annular) lid is placed on top of the bulk solid specimen. The lid is fixed at a cross-beam.

A normal force,  $F_N$ , is exerted to the crossbeam in the rotational axis of the shear cell and transmitted through the lid to the bulk solid specimen. Thus, a normal stress  $\sigma$  is applied to the bulk solid specimen. The counterbalance force,  $F_A$ , also acts in the centre of the crossbeam.  $F_A$  is directed upward and is created by counterweights.  $F_A$  counteracts the gravity forces of the lid, the hanger, and the crossbeam.

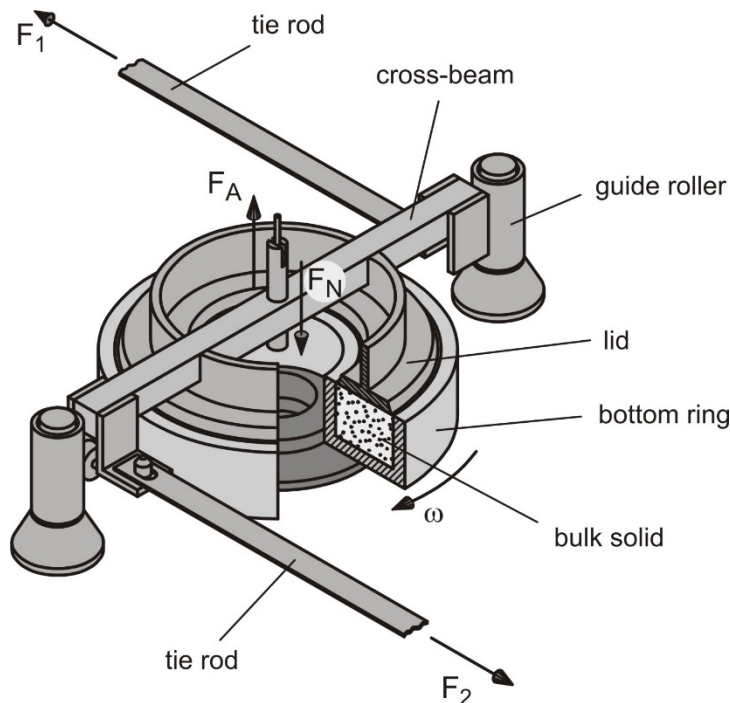


**Fig. 12:** Shear cell of a ring shear tester (here: Ring Shear Tester type RST-01.pc) [6, 9, 10, 13]

To shear the bulk solid, the lid and the bottom ring of the shear cell must rotate relative to each other. This is accomplished by rotating the bottom ring in the direction of the arrow  $\omega$  ( $\omega$  is the angular velocity), whereas the lid and the crossbeam are prevented from rotation by two tie-rods connected to the crossbeam. Each of the tie-rods is fixed at a load beam, so that the forces,  $F_1$  and  $F_2$ , acting in the tie rods can be measured.

The bottom of the shear cell and the lower side of the lid are rough in order to prevent the bulk solid from sliding relative to these surfaces. Therefore, rotation of the bottom ring relative to the lid creates a shear deformation within the bulk solid. Through this shearing the bulk solid is deformed and thus a shear stress  $\tau$  prevails. The forces acting in the tie rods ( $F_1$  and  $F_2$ ) are directly proportional to the shear stress  $\tau$  acting in the bulk solid.

In addition to the shear force ( $F_1, F_2$ ), the ring shear tester also measures the vertical position of the lid. If a bulk solid is compressible, its bulk density,  $\rho_b$ , increases depending on the normal load applied. Knowing the vertical position of the lid, volume and bulk density of the bulk solid specimen can be calculated.

The principle of the ring shear tester described above is different from other ring shear testers in a few important details, e.g. the lid, which lies on the bulk solid sample, similar to the lid of the Jenike shear cell, and is not held horizontally by a bearing as with older ring shear testers. This yields a more homogeneous stress distribution across the specimen, and the absence of any bearing friction increases the accuracy of the measurement. Additionally, the masses of the lid and all parts connected to it are small, so that tests at low normal stresses are possible, and the shear cell including the lid and the bulk solid specimen can be taken from the tester without disturbing the sample, e.g. for time consolidation tests using a time consolidation bench.

The test procedure (Fig. 13) is quite similar to the test procedure recommended for the Jenike Tester (preshear and shear, see above), although the test procedure for the ring shear tester is less time consuming, easier to perform, and, hence, less influenced by the person who runs the test. This in combination with the design outlined in the last paragraph results in the good reproducibility compared to other testers [6, 18, 19].

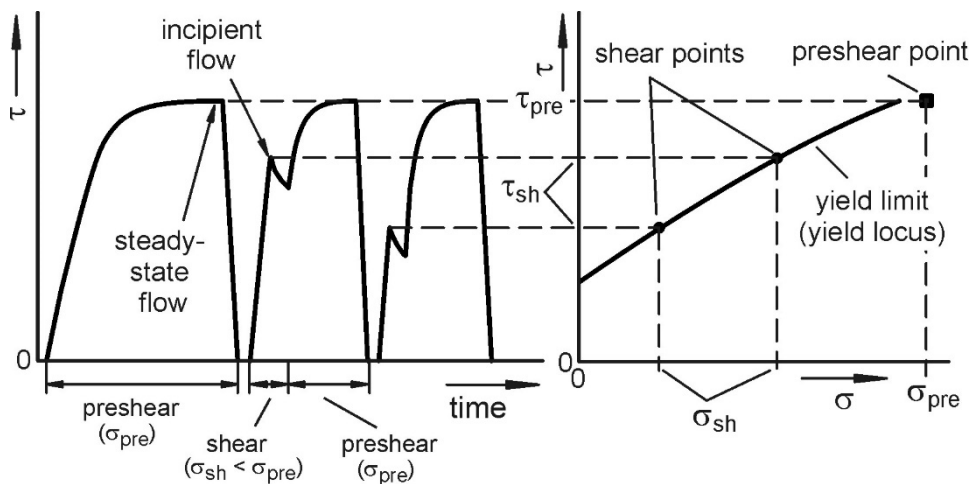


**Fig. 13:** Shear test procedure of a ring shear tester

With the ring shear tester usually a complete yield locus is measured with one specimen (in contrast to the Jenike Tester where only one point can be measured with one specimen). In order to measure another point of the yield locus with the same specimen, after shear (shear to failure) the normal stress is increased again to  $\sigma_{pre}$ , which is the normal stress applied at first preshear. Then the specimen is presheared again under this normal stress until steady-state flow is attained. Thus, the specimen is again critically consolidated. After the specimen is relieved from shear stress (backward rotation of the shear cell until  $\tau = 0$ ), the normal stress is reduced to another value of  $\sigma_{sh} < \sigma_{pre}$  (Fig. 13), and the specimen is then sheared again, thus obtaining another point of the yield locus in the  $\sigma, \tau$ -diagram. After shear, the specimen is again presheared, then sheared, and so on, until a sufficient number of points of the yield locus are known and the yield locus can be drawn.

## 5.4 Yield locus

The parameters which describe the flow properties can be determined from the yield locus (Fig. 14). The relevant consolidation stress  $\sigma_1$  is equal to the major principal stress of the Mohr stress circle which is tangential to the yield locus and intersects at the point of steady state flow ( $\sigma_{pre}, \tau_{pre}$ ). This stress circle represents the stresses in the sample at the end of the consolidation procedure (stresses at steady state flow). It corresponds to the stress circle at the end of consolidation at the uniaxial compression test (Fig. 3). The unconfined yield strength,  $\sigma_c$ , results from the stress circle which is tangential to the yield locus and which runs through the origin (minor

principal stress  $\sigma_2 = 0$ ). This stress circle represents a similar stress state as the one which prevails in the second step of the uniaxial compression test (stress circle B<sub>3</sub>, Fig. 6). In contrast to the uniaxial compression test the unconfined yield strength,  $\sigma_c$ , has to be determined on basis of the yield locus and does not follow directly from the measurement.

Please note that the analogy between the uniaxial compression test and the shear test is used here for the explanation of the yield locus. In reality, the stress circles at uniaxial compression and at steady state flow are not exactly the same, and a uniaxial compression test usually results in a smaller unconfined yield strength than a shear test [5, 6, 20, 21].

A straight line through the origin of the  $\sigma, \tau$ -diagram, tangent to the greater Mohr circle (steady-state flow), is the effective yield locus as defined by Jenike [1] (broken line in Fig. 14). It encloses the  $\sigma$ -axis with the angle  $\varphi_e$  (effective angle of internal friction). Because the largest Mohr stress circle indicates a state of steady-state flow, the angle  $\varphi_e$  can be regarded as a measure of the internal friction at steady-state flow. This angle is required for silo design according to Jenike's theory.

Further quantities resulting from a yield locus test are the angle of internal friction which is approximated by the slope angle,  $\varphi_{lin}$ , of the linearized yield locus, and the bulk density at the state of consolidation which is determined from the mass and volume of the consolidated specimen [6].

If several yield loci are measured at different stress levels, i.e., with different normal stresses at preshear,  $\sigma_{pre}$ , each yield locus represents another state of consolidation and another bulk density. The above-mentioned flow properties (unconfined yield strength, effective angle of internal friction) can be indicated as a function of the consolidation stress,  $\sigma_1$ , similar to Fig. 4 where bulk density and unconfined yield strength are plotted vs. the consolidation stress.

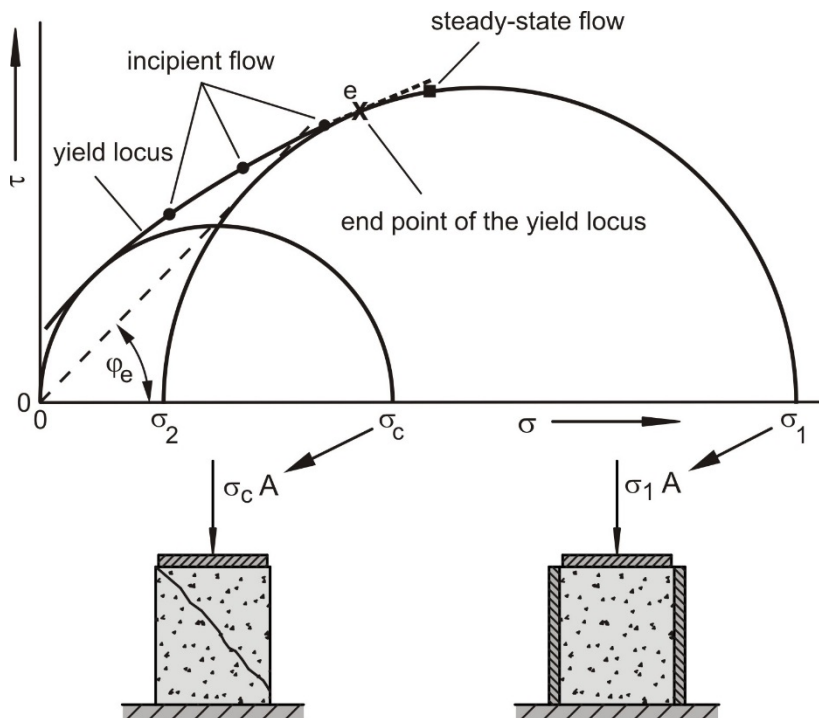


**Fig. 14:** Yield locus, analogy to uniaxial compression test

## 5.5 Time consolidation

The effect of time consolidation has been outlined in Section 4.2.

Time consolidation, which results in the increase of the unconfined yield strength with time during storage at rest, is measured with a shear tester like the measurement of a yield locus. First a bulk solid specimen is presheared (consolidated). After preshear the specimen is stored for a period,  $t$ , under the vertically acting normal stress,  $\sigma$ , which is selected to be equal to the consolidation stress,  $\sigma_1$ , of the corresponding yield locus (a yield locus must be measured prior to the time consolidation tests). This ensures that during the consolidation period the same major principal stress (= consolidation stress,  $\sigma_1$ ) acts on the specimen as during steady-state flow at preshear.

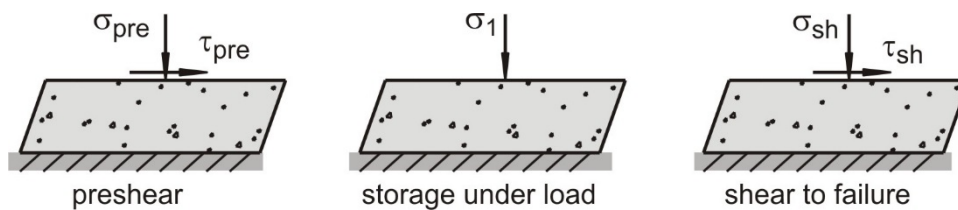


**Fig. 15:** Time consolidation test

After the time consolidation period  $t$  the specimen is sheared to failure. For this, a vertical normal load,  $\sigma_{sh} < \sigma_1$ , is selected. As with shear without time consolidation (measurement of a point of a yield locus), so also after time consolidation will one observe a shear stress maximum (Fig. 16). If consolidation time affects the bulk solid under consideration, after the consolidation period the shear stress maximum will be larger than it would have been without a consolidation period between preshear and shear.

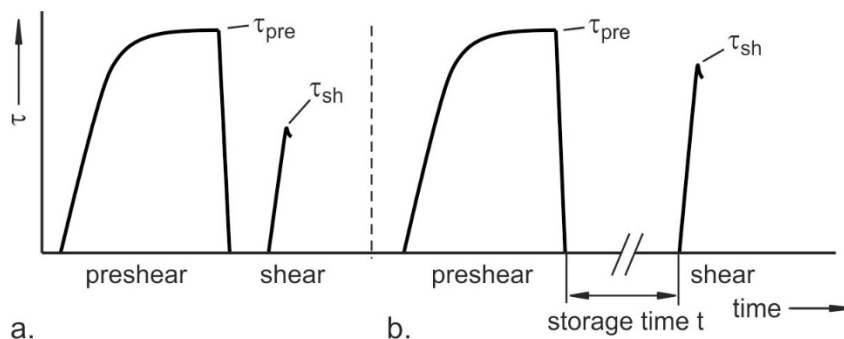


**Fig. 16:** Shear stress vs. time at shear; with (a) and without (b) storage for time consolidation

The maximum shear stress,  $\tau_{sh}$ , is a point of a yield limit, which is valid for the applied storage period,  $t$ , and called a “time yield locus”. Figure 17 shows a yield locus and two time yield loci obtained for different consolidation periods,  $t_1$  and  $t_2$ . The yield locus can also be regarded as a time yield locus for  $t = 0$ .



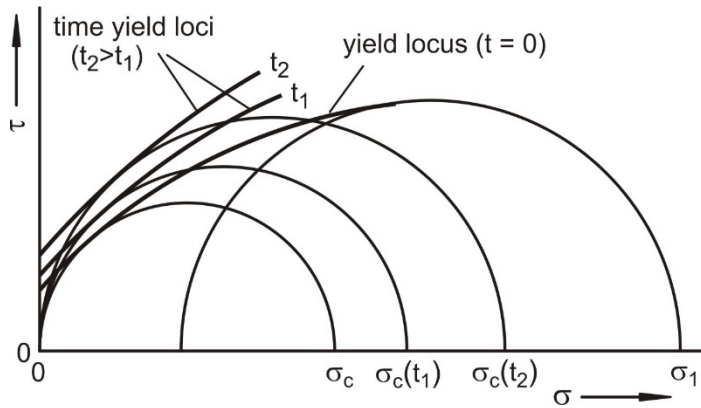


**Fig. 17:** Yield locus and time yield loci

With the measured shear points a time yield locus can be approximated similarly to the approximation of a yield locus. Compared to the yield locus, the time yield locus is shifted towards greater shear stresses,  $\tau$  (if the bulk solid shows an increase of strength with time). The unconfined yield strength,  $\sigma_c$ , is determined in the same way as for a yield locus by drawing a Mohr stress circle through the origin and tangent to the time yield locus. In Fig. 17 the values of the unconfined yield strength for the consolidation periods,  $t_1$  and  $t_2$ , are designated as  $\sigma_c(t_1)$  and  $\sigma_c(t_2)$ .

Time yield loci can be determined for different storage periods (consolidation periods). Each time yield locus is valid for only one consolidation period and one consolidation stress. If the strength of the bulk solid increases over time, the time yield loci will be shifted towards larger values of  $\tau$  as the consolidation period,  $t$ , increases (see Fig. 17,  $t_2 > t_1$ )

## 5.6 Wall friction

Wall friction is the friction between a bulk solid and the surface of a solid, e.g. the wall of a silo or a bin. The coefficient of wall friction or the wall friction angle, respectively, is important both for silo design for flow and silo design for strength, but also for the design of chutes and other equipment, where the bulk solid will flow across a solid surface. Knowing the wall friction angle, it is possible to decide whether the polishing of the wall surface or the use of a liner would have advantages in the flow of the bulk solid.

The principle of a wall friction test, where the kinematic angle of wall friction is determined, is shown in Fig. 18. The bulk solid specimen is subjected to a vertical normal stress. The normal stress acting between bulk solid specimen and wall material is called the wall normal stress,  $\sigma_w$ .

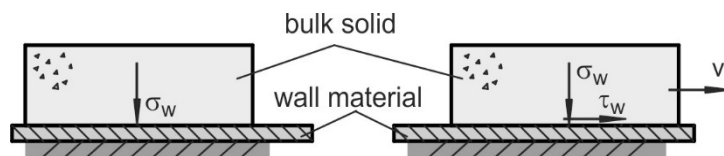


**Fig. 18:** Principle of a wall friction test

The bulk solid specimen is then shifted relative to the wall material surface with a constant velocity,  $v$ . This process is called shear (similar to the yield locus test). The shear stress acting between bulk solid specimen and wall material is measured.

It is usual to measure wall friction at incrementally decreasing wall normal stresses [4, 7, 8]. Thus, one begins with the greatest wall normal stress ( $\sigma_{w1}$  in Fig. 19). At the beginning of the shear process the wall shear stress,  $\tau_w$ , increases. With time, the increase of the wall shear stress becomes less until finally a constant wall shear stress,  $\tau_{w1}$ , is attained (steady-state shear

stress). The constant wall shear stress,  $\tau_{w1}$ , is characteristic for the applied wall normal stress,  $\sigma_{w1}$ . After the steady-state condition is attained, the normal load is reduced. With each decrease in wall normal stress, wall shear stress,  $\tau_w$ , also decreases (Fig. 19). After a certain time, a steady-state shear stress is again attained. In this way values of steady-state wall friction at several wall normal stresses are measured.

The pair of values of wall normal stress and constant wall shear stress ( $\sigma_w, \tau_w$ ) describes the kinematic wall friction at the wall normal stress,  $\sigma_w$ , and is used for the evaluation of the test. All pairs of values of wall normal stress and steady-state wall shear stress are plotted in a  $\sigma_w, \tau_w$ -diagram (Fig. 19, right). The curve (or line) running through the measured points is called the wall yield locus.

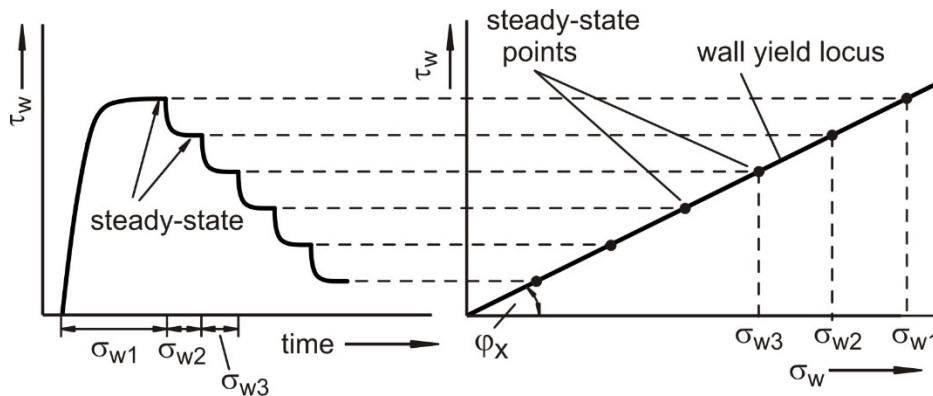


**Fig. 19:** Course of wall shear stress in a wall friction test; wall yield locus

The wall yield locus is a yield limit like the yield locus. The wall yield locus describes the wall shear stress,  $\tau_w$ , necessary to shift a bulk solid continuously across a wall surface under a certain wall normal stress,  $\sigma_w$ . Since the wall yield locus is based on the shear stresses measured at steady-state conditions, it describes the kinematic friction of the bulk solid. Thus, the wall yield locus could more exactly be called a kinematic wall yield locus [7, 8].

To quantify wall friction, the wall friction angle,  $\varphi_x$ , or the coefficient of wall friction,  $\mu$ , are used. The larger the wall friction angle or coefficient of wall friction, the greater is wall friction. The coefficient of wall friction,  $\mu$ , is the ratio of wall shear stress,  $\tau_w$ , to wall normal stress,  $\sigma_w$ . The wall friction angle,  $\varphi_x$ , is the slope of a line running through the origin of the  $\sigma_w, \tau_w$ -diagram and a point of the wall yield locus.

If the wall yield locus is a straight line running through the origin (Fig. 19), the ratio of wall shear stress,  $\tau_w$ , to wall normal stress,  $\sigma_w$ , has the same value for each point of the wall yield locus. Thus, one obtains the identical wall friction coefficient,  $\mu$ , and the identical wall friction angle,  $\varphi_x$ , for each point of the wall yield locus. In this case wall friction is independent of wall normal stress.

The wall yield locus shown in Fig. 20 is curved and does not run through the origin. In this case one finds a different wall friction coefficient and wall friction angle for each point of the wall yield locus. Thus, the wall friction coefficient and the wall friction angle are dependent on wall normal stress,  $\sigma_w$ . This can be seen by the wall friction angles,  $\varphi_{x1}$  and  $\varphi_{x2}$ , which follow for the wall normal stresses,  $\sigma_{w1}$  and  $\sigma_{w2}$ . A wall yield locus intersecting the  $\tau$ -axis at  $\tau_{ad} > 0$  is typical for materials tending to adhere at walls (e.g. like moist clay). The shear stress,  $\tau_{ad}$ , at the point of intersection is called adhesion.

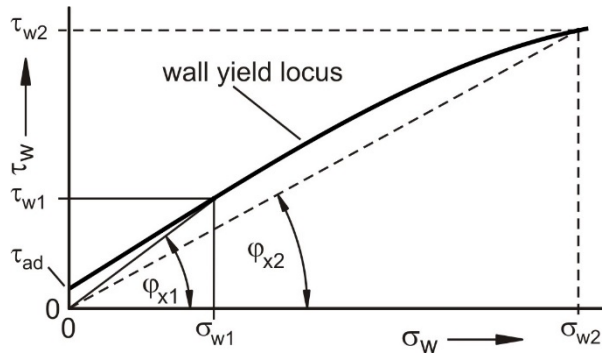


**Fig. 20:** Wall yield locus; wall friction angle is dependent on the wall normal stress.

Wall friction can be measured with the shear testers described above. The setup of the Jenike shear tester for a wall friction test is shown in Fig. 21. The bottom ring of the shear cell is replaced by a sample of wall material (e.g. stainless steel, coated steel). The wall normal stress is then adjusted by the normal force,  $F_N$ , and the shear force,  $F_S$ , is measured following the procedure outlined above.

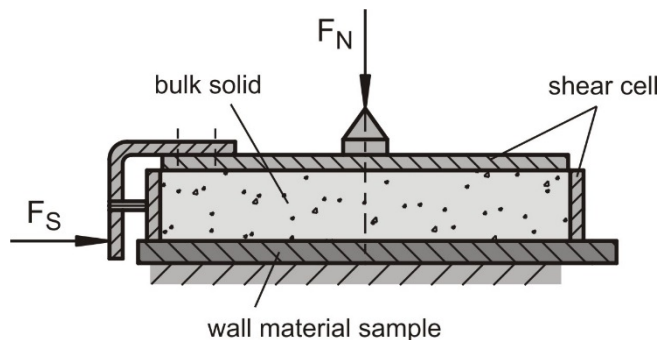


**Fig. 21:** Measurement of wall friction with the Jenike shear tester [4, 7, 8]

Figure 22 shows the setup of the wall friction shear cell of the Schulze ring shear tester [6, 9, 10, 13]. The annular bottom ring contains the sample of the wall material. On top of the wall material sample is the bulk solid specimen, which is covered with the annular lid of the shear cell. The lid is connected to the crossbeam. Except for the geometry of bottom ring and lid, the setup is similar to the setup of the shear cell for flow properties testing (Section 5.3).

To measure wall friction the shear cell is rotated slowly in the direction of arrow  $\omega$ , while the lid is prevented from rotating by the two tie rods. The forces acting on the tie rods,  $F_1$  and  $F_2$ , are measured. The layer of bulk solid located between the lid and the surface of the wall material sample is prevented from rotating by the lid, which has a rough underside. Thus, the bulk solid is shifted across the surface of the wall material sample while it is subjected to the normal stress,  $\sigma_w$ . The wall shear stress,  $\tau_w$ , is calculated from the  $F_1$  and  $F_2$ .

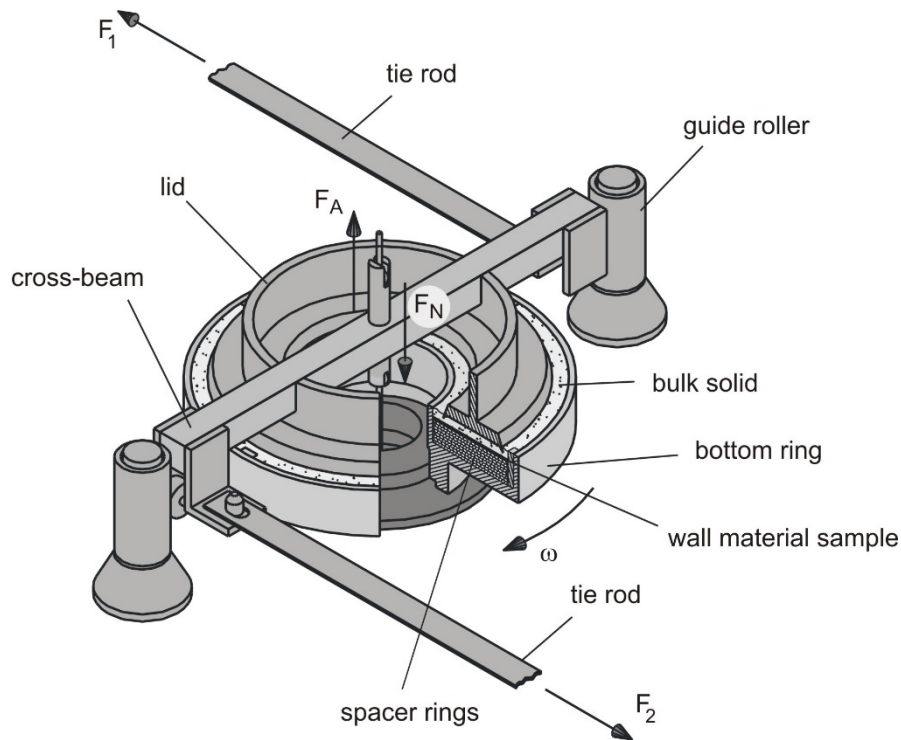


**Fig. 22:** Setup of the shear cell for wall friction tests (Schulze ring shear tester) [6, 9, 10, 13]

## 6 Summary

Consolidated bulk solids have yield limits like other materials. These yield limits, which can be measured with shear testers, are called yield loci. They depend on the consolidation which has previously taken place and, sometimes, also on the storage time. If a bulk solid is to be set in motion, e.g. to flow out of a silo, the stresses acting on the bulk solid must be large enough to ensure that the corresponding Mohr stress circle touches the yield locus of the consolidated bulk solid.

The flow properties which can be obtained from the measured yield loci are exactly defined physical figures. Unconfined yield strength (dependent on consolidation stress and storage time), bulk density, and wall friction angle are the most important flow properties for the design of storage and conveying systems as well as for comparative tests, quality control, and product development.

## References

- [1] Kwade, A.; Schulze, D.; Schwedes, J.: Determination of the stress ratio in uniaxial compression tests, *Powder Handling & Processing* 6 (1994) 1, pp. 199–203
- [2] Molerus, O.: *Schüttgutmechanik*, Springer Verlag, Berlin – Heidelberg – New York – Tokyo (1985)
- [3] Tomas, J., Schubert, H.: Fließverhalten von feuchten Schüttgütern, *Aufbereitungstechnik* (1985) 7, S. 399–404
- [4] Jenike, A.W.: *Storage and flow of solids*, Bull. No. 123, Engng. Exp. Station, Univ. Utah, Salt Lake City (1964)
- [5] Schwedes, J., Schulze, D.: Measurement of flow properties of bulk solids, *Powder Technology* 61 (1990), pp. 59–68
- [6] Schulze, D.: *Powders and Bulk Solids – Behavior, Characterization, Storage and Flow*, Springer Berlin – Heidelberg – New York – Tokyo, 2<sup>nd</sup> ed. (2021)
- [7] The Institution of Chemical Engineers (Eds.): *Standard shear testing technique for particulate solids using the Jenike shear cell* (1989)
- [8] ASTM Standard D6128: *Standard Test Method for Shear Testing of Bulk Solids Using the Jenike Shear Tester* ASTM International, [www.astm.org](http://www.astm.org)
- [9] Schulze, D.: Development and application of a novel ring shear tester, *Aufbereitungstechnik* 35 (1994) 10, pp. 524–535
- [10] Schulze, D.: A new ring shear tester for flowability and time consolidation measurements, *Proc. 1st International Particle Technology Forum*, August 1994, Denver, Colorado, USA, pp. 11–16
- [11] Schulze, D.: Appropriate devices for the measurement of flow properties for silo design and quality control, *PARTEC 95*, Preprints “3rd Europ. Symp. Storage and Flow of Particulate Solids“, 21.–23.3.95, Nürnberg, pp. 45–56
- [12] Schulze, D.: Flowability and time consolidation measurements using a ring shear tester, *Powder Handling & Processing* 8 (1996) 3, pp. 221–226
- [13] ASTM Standard D6773: *Standard shear test method for bulk solids using the Schulze ring shear tester*, ASTM International, [www.astm.org](http://www.astm.org)
- [14] Hvorslev, M.J.: Über die Festigkeitseigenschaften gestörter bindiger Böden, *Ingeniørvidenskabelige Skrifter A*, No. 45 (1939)
- [15] Carr, J.F., Walker, D.M.: An annular shear cell for granular materials, *Powder Technology* 1 (1967/68), pp. 369–373
- [16] Gebhard, H.: Scherversuche an leicht verdichteten Schüttgütern unter besonderer Berücksichtigung des Verformungsverhaltens, *Diss. Univ. Karlsruhe* (1982)
- [17] Münz, G.: Entwicklung eines Ringschergerätes zur Messung der Fließigenschaften von Schüttgütern und Bestimmung des Einflusses der Teilchengrößenverteilung auf die Fließigenschaften kohäsiver Kalksteinpulver, *Diss. Univ. Karlsruhe* (1976)
- [18] Verlinden, A.: *Experimental assessment of shear testers for measuring flow properties of bulk solids*, PhD-Thesis, Univ. of Bradford, UK (2000)
- [19] Schulze, D.: Round Robin Test on Ring Shear Testers, *Advanced Powder Technology* 22 (2011) 2, pp. 197–202
- [20] Schulze, D.: Flowability of bulk solids – Definition and measuring techniques, Part I and II, *Powder and Bulk Engineering* 10 (1996) 4, pp. 45–61, and 10 (1996) 6, pp. 17–28
- [21] Schulze, D.: The measurement of the flowability of bulk solids. In: Brown CJ, Nielsen J (Eds.) *Silos – Fundamentals of theory, behaviour and design*. E & FN Spon, London und New York (1998), pp. 18–52